Nmp4/CIZ Suppresses the Parathyroid Hormone Anabolic Window by Restricting Mesenchymal Stem Cell and Osteoprogenitor Frequency

Yongzheng He,[1,2,*] Paul Childress,[3,*] Mark Hood, Jr.,[3] Marta Alvarez,[3] Melissa A. Kacena,[4] Michael Hanlon,[3,†] Bryce McKee,[3] Joseph P. Bidwell,[3] and Feng-Chun Yang[1–3]

Parathyroid hormone (PTH) anabolic osteoporosis therapy is intrinsically limited by unknown mechanisms. We previously showed that disabling the transcription factor Nmp4/CIZ in mice expanded this anabolic window while modestly elevating bone resorption. This enhanced bone formation requires a lag period to materialize. Wild-type (WT) and *Nmp4*-knockout (KO) mice exhibited equivalent PTH-induced increases in bone at 2 weeks of treatment, but by 7 weeks, the null mice showed more new bone. At 3-week treatment, serum osteocalcin, a bone formation marker, peaked in WT mice, but continued to increase in null mice. To determine if 3 weeks is the time when the addition of new bone diverges and to investigate its cellular basis, we treated 10-week-old null and WT animals with human PTH (1–34) (30 μg/kg/day) or vehicle before analyzing femoral trabecular architecture and bone marrow (BM) and peripheral blood phenotypic cell profiles. PTH-treated *Nmp4*-KO mice gained over 2-fold more femoral trabecular bone than WT by 3 weeks. There was no difference between genotypes in BM cellularity or profiles of several blood elements. However, the KO mice exhibited a significant elevation in CFU-F cells, CFU-F$^{AlkPhos+}$ cells (osteoprogenitors), and a higher percentage of CFU-F$^{AlkPhos+}$ cells/CFU-F cells consistent with an increase in CD45−/CD146+/CD105+/nestin+ mesenchymal stem cell frequency. Null BM exhibited a 2-fold enhancement in CD8+ T cells known to support osteoprogenitor differentiation and a 1.6-fold increase in CFU-GM colonies (osteoclast progenitors). We propose that Nmp4/CIZ limits the PTH anabolic window by restricting the number of BM stem, progenitor, and blood cells that support anabolic bone remodeling.

Introduction

Anabolic therapy is the preferred pharmacological intervention for osteoporosis [1], and parathyroid hormone (PTH) is the only FDA-approved drug that adds bone to the osteoporotic skeleton; however, its bone-forming activity, or anabolic window is intrinsically limited to about 2 years, thereafter falling to baseline [2–5]. Therefore, PTH is not approved as a long-term osteoporosis therapy, and its use is indicated only for those patients who are at a high risk of fractures or who are unresponsive to other available therapies [6].

While the mechanisms regulating the extent of the PTH anabolic window are unknown, we demonstrated that disabling the transcription factor nuclear matrix protein 4/cas-interacting zinc-finger protein (Nmp4/CIZ) in mice significantly extends and augments PTH bone-forming capacity;

treatment of wild-type (WT) and *Nmp4*- knockout (KO) mice with intermittent PTH for 7 weeks resulted in significant increases in serum osteocalcin, a marker for bone formation, but these serum profiles as a function of time were strikingly different [7,8]. In the WT mice, serum osteocalcin peaked at 3 weeks of treatment and returned to baseline by 7 weeks of hormone administration [7]. However, in the null mice, this PTH-induced surge in serum osteocalcin exceeded that observed in the WT mice and was still climbing at the end of the 7-week treatment regimen [7]. Consistent with this sustained serum osteocalcin surge, at the end of the 7-week treatment period, the null mice had gained significantly more femoral, vertebral, and tibial trabecular bone than WT mice while maintaining robust increases in cortical bone [7,8]. These enhanced increases in cancellous bone in the *Nmp4*-KO skeleton all showed significant treatment×genotype

---

[1]Department of Pediatrics, Indiana University School of Medicine, Indianapolis, Indiana.
[2]Herman B Wells Center for Pediatric Research, Indianapolis, Indiana.
Departments of [3]Anatomy & Cell Biology and [4]Orthopaedic Surgery, Indiana University School of Medicine, Indianapolis, Indiana.
*These authors contributed equally to this work.
†Present affiliation: Iowa State University College of Veterinary Medicine, Ames, Iowa.

interactions, thus demonstrating that Nmp4/CIZ suppresses PTH-stimulated anabolism [7,8].

When in the PTH treatment regimen does bone formation in the Nmp4-KO mice eclipse WT growth, and what sustains this extended and enhanced anabolic activity? The WT and Nmp4-KO mice exhibited equivalent PTH-induced increases in trabecular bone during the first 2 weeks of treatment; however, at this treatment point, femoral mRNA profiles revealed a transient enhanced increase in PTH-stimulated c-fos and Fra-2 expression in the null mice as well as an elevated expression of Nfatc1 in these animals [7]. Although these transcription factors mediate numerous functions within the context of bone, this is consistent with an enhanced PTH-induced increase in mesenchymal stem cell self-renewal and/or recruitment of null osteoblasts and osteoclasts into the anabolic window [9–13]. Interestingly, the untreated Nmp4-KO mice had a modest, but significantly elevated, bone mineral density and bone mineral content as compared to WT animals [8] despite modestly elevated levels of serum C-terminal telopeptides of type I collagen (CTX), a marker for bone resorption [7]. The Nmp4-KO bone marrow (BM) yielded ~1.8-fold more osteoclasts in vitro as compared to WT marrow, and the null osteoclasts were significantly more active than their WT counterparts [7]. Therefore, bone formation was exceeding resorption, but how this occurred was not clear (eg, osteoblast–osteoclast coupling [14] and/or intrinsic differences in stem and progenitor pools that support bone formation or resorption).

To address whether the enhanced PTH-stimulated addition of trabecular bone in the Nmp4-KO mice is coincident with the initial surge in the serum osteocalcin, and to determine the cellular basis of this sustained enhanced anabolic activity, we treated WT and Nmp4-KO female mice with intermittent PTH for 3 weeks before harvesting femurs, femoral BM, and peripheral blood (PBL). Our data reveal that the Nmp4-KO mice show significantly enhanced PTH-stimulated addition of trabecular bone at 3 weeks of hormone treatment, and that Nmp4 has a profound regulatory role in BM population dynamics. Disabling this transcription factor results in alterations in stem, progenitor, and blood cell populations that accommodate the prolongation of the PTH anabolic window while maintaining bone remodeling. These data reveal novel aspects of how the PTH anabolic window is regulated and have implications for a novel adjuvant osteoporosis therapy.

Materials and Methods

Mice

Nmp4-KO mice, backcrossed onto a C57BL/6J background for 6–7 generations, [7,8], and their WT littermates were used for these studies. Our local Institutional Animal Care and Use Committee approved all experiments and procedures involving the production and use of the mice described in this investigation.

PTH treatment

Before initiating hormone treatment, 8-week-old female WT and Nmp4-KO mice were given 100 μL sterile saline by subcutaneous (sc) injection, once daily to habituate them to handling. At 10 weeks of age, animals were sorted into 4 treatment groups based on equivalent mean-group–body weight. These 4 groups included (1) vehicle-treated WT; (2) PTH-treated WT; (3) vehicle-treated Nmp4-KO, and (4) PTH-treated Nmp4-KO mice. Experimental animals were injected sc with human PTH 1–34 [hPTH(1–34), Bachem Bioscience, Inc.] at 30 μg/kg/day, daily or vehicle control (0.2% BSA/0.1% 1.0 mN HCl in saline; Abbott Laboratory) for 3 weeks. There was no significant difference in initial and final mean-group-body weights between genotypes. In a separate experiment, the BM of untreated female WT and Nmp4-KO mice (13 weeks of age) was harvested to compare the multipotent mesenchymal stem cell (CD45 − /CD146 + /CD105 + /nestin +) frequency.

CFU-F$^{AlkPhos+}$ assay [15]

BM was flushed from femurs; single-cell suspensions were prepared, and cells were seeded into 6-well plates at an initial density of 1×10^6 cells/well. Each culture well contained 2 mL of complete α-MEM supplemented with 100 IU/mL penicillin, 100 μg/mL streptomycin, 25 μg/mL amphotericin, 2 mM L-glutamine (Hyclone Laboratories, Inc.), ascorbic acid (50 μg/mL, Sigma), and 10% fetal bovine serum (FBS; Atlanta Biologicals). The medium was changed every 2 days for 14 days. Subsequently, cells were fixed and stained for alkaline phosphatase using a Sigma-Aldrich Alkaline Phosphatase Staining Kit and then counted for colony-forming units—fibroblastic/alkaline phosphatase+ (CFU-F$^{AlkPhos+}$). Colonies were defined as positive staining with 25 or more cells per colony. After counting CFU-F$^{AlkPhos+}$ colonies, the cells were stained with crystal violet, and all colonies were counted for total CFU-F.

Flow cytometry

Whole BM was isolated by flushing the femurs of experimental mice with α-MEM supplemented with 10% FBS. PBL was collected from the mice by cardiac puncture. The red blood cells (RBCs) were lysed with an RBC lysis buffer (Qiagen) before the PBL and BM were processed for flow cytometric analysis. All antibodies for flow cytometry were purchased from BD Biosciences. Stained samples were analyzed on an FACS Caliber (BD Biosciences), and results were quantified using FlowJo Version 8.8.6 software (Tree Star, Inc.).

Clonogenic assays

Colony-forming units (CFU-Cs) were assayed as previously described [16]. Briefly, 2.5×10^4 BM mononucleated cells or 25 μL PBL was seeded onto a 35-mm gridded dish containing methylcellulose and murine stem cell factor (100 ng/mL), murine granulocyte–macrophage colony-stimulating factor (10 ng/mL), murine interleukin 3 (IL3, 5 ng/mL), murine recombinant macrophage–colony stimulating factor (10 ng/mL), and human erythropoietin (4 U/mL) for 7 days at 37°C in a 5% CO_2 incubator. Colonies were scored using an inverted light microscope. All cytokines were purchased from PeproTech.

Hemavet analysis

PBL was collected from the WT and Nmp4-KO mice and processed for blood cell enumeration using the Hemavet 950

FS according to the manufacturer's instructions (Drew Scientific).

Micro computed tomography

We previously reported no differences in the femur length between *Nmp4*-KO and WT mice at 8 and 17 weeks of age [8]. Therefore, after euthanasia, a 2.6-mm span ($\sim 5\,mm^3$ of medullary space) of the distal femoral metaphysis was scanned in 70% ethanol on a desktop microcomputed tomography (μCT) (μCT 35; Scanco Medical AG) at 10-μm resolution using 55-kVp tube potential and 400-ms integration time to measure trabecular three-dimensional (3D) morphometric properties as previously described [17]. From the 3D constructs, trabecular bone volume per total volume (BV/TV, %), connectivity density (Conn.D, mm^{-3}), structure model index (SMI), trabecular number (Tb.N, mm^{-1}), trabecular thickness (Tb.Th, mm), and spacing (Tb.Sp, mm) were calculated using Scanco software.

Statistical analysis

The program JMP version 7.0.1 (SAS Institute) was used to process all statistical evaluations. We employed a 2-way analysis of variance (ANOVA) for the PTH studies using genotype and treatment as the independent variables. If a genotype×treatment interaction was indicated, the data were analyzed by a Tukey honestly significant difference (HSD) post hoc test to determine significant differences between the experimental groups. Statistical significance was set at $P \leq 0.01$ to guard against type I errors. A separate experiment was conducted using a distinct group of our experimental mice for the purpose of comparing the frequency of multipotent mesenchymal stem cells (CD45 – /CD146 + /CD105 + /nestin +) in untreated female WT and *Nmp4*-KO mice. These data were analyzed with a 2-sample *t*-test, assuming unequal variances and statistical significance was set at $P \leq 0.05$. The numbers of mice per treatment group are indicated in the appropriate Figures and Tables.

Results

Nmp4-KO mice exhibited an enhanced increase in femoral trabecular bone after 3 weeks of treatment

To determine if the divergence between the WT and *Nmp4*-KO mice in serum osteocalcin levels at 3 weeks is coincident with the beginning of the enhanced addition of trabecular bone in the null animals observed at 7 weeks [7], we sorted WT and *Nmp4*-KO mice into 4 treatment groups and harvested the femurs for μCT analysis as described in the Materials and Methods section. Although the WT and null mice had previously shown equivalent PTH-induced increases in trabecular bone at 2 weeks of treatment [7], in the present study, the null mice exhibited significantly augmented PTH-stimulated increase in femoral trabecular bone as compared to their WT littermates at 3 weeks (Fig. 1). The *Nmp4*-null mice showed a more robust PTH-stimulated increase in BV/TV compared to the WT animals during the first 3 weeks of treatment (Fig. 1A). The KO mice added ~ 2.3-fold more bone than their WT littermates in response to PTH (Fig. 1A). The 2-way ANOVA indicated a strong ge-

notype×treatment interaction, and the Tukey HSD post hoc determined that there was no difference in BV/TV between the vehicle-treated WT and KO animals (Fig. 1A). While PTH treatment increased connectivity parameters (Conn.D, mm^{-3}) for both genotypes, a significantly greater enhancement was observed in *Nmp4*-KO mice compared to WT mice (Fig. 1B). Again, there was no difference between the vehicle-treated WT and null mice. The SMI was used to evaluate the PTH-induced alteration in femoral trabecular morphology. This parameter measures changes from a rod-like to a plate-like form, and the lower the value, the more plate-like the shape, which is indicative of an increase in bone strength [18]. PTH treatment of both WT and *Nmp4*-KO mice resulted in a significant transition to a more plate-like morphology, which was more pronounced in the null mice with a significant genotype×treatment effect (Fig. 1C). Interestingly, the SMI value for the femoral bone of the KO mice treated with vehicle was statistically equivalent to that of the WT mice treated with PTH (Fig. 1C). While PTH treatment significantly increased trabecular thickness (Tb.Th, mm, Fig. 1D) in null mice, treatment did not alter trabecular thickness in WT mice. Finally, PTH equivalently increased the trabecular number (Tb.N, mm^{-1}, Fig. 1E) and decreased spacing (Tb.Sp, mm, Fig. 1F) in both genotypes.

BM cellularity, spleen weight, and the profiles of most blood elements did not differ between the WT and Nmp4-KO mice

To address whether there are differences between the *Nmp4*-null and WT mice in the BM or PBL cellular profiles supportive of the observed enhanced PTH-induced addition of trabecular bone, we obtained immunophenotypic, clonogenic, and hematological profiles at 3 weeks of treatment (Tables 1–3). The spleen weight measured, as a% of total body weight, did not differ with the genotype, but did modestly increase with PTH treatment in both WT and null mice (Table 1). The profiles of blood elements between the *Nmp4*-KO and WT mice were unremarkable. We observed no differences between any of the treatment groups in the BM and PBL profiles of the RBCs, WBCs, platelets, neutrophils, lymphocytes, eosinophils, monocytes, B-cell lineages, CD4 + T cells, or the Lin(-)Sca-1(+)c-Kit(+) (LSK) cells (Tables 1 and 2). Finally, there were no differences between WT and *Nmp4*-KO mice in CFU-C, CFU-G, CFU-GEMM, and CFU-M cells (Table 3). PTH treatment had no impact on any of these parameters (Tables 1–3).

Nmp4-KO BM yielded more multipotent MSCs (CD146+/nestin+), CFU-F$^{AlkPhos+}$, CFU-GM, and CD8+ T cells than WT BM

To determine if the source of this augmented bone formation in *Nmp4*-null mice is derived, in part, from an expanded pool of osteoprogenitors, we obtained BM from our experimental groups for analysis of CFU-F$^{AlkPhos+}$ colonies as described in the Materials and Methods section. We recovered ~ 4-fold more CFU-F$^{AlkPhos+}$ colonies from the null mice than the WT animals (Fig. 2A). The total number of CFU-F colonies was significantly elevated in the *Nmp4*-KO cultures (Fig. 2B), and the percentage of CFU-F$^{AlkPhos+}$/total CFU-F colonies was significantly increased in the cultures

A

2W ANOVA | Prob>ltl
GENOTYPE | <0.0001
TREATMENT | <0.0001
TREAT X GENE | <0.0001
TUKEY HSD
KO PTH | A
WT PTH | B
KO VEH | BC
WT VEH | C
Groups not connected by the same letter are different

B

2W ANOVA | Prob>ltl
GENOTYPE | <0.0001
TREATMENT | <0.0001
TREAT X GENE | <0.0001
TUKEY HSD
KO PTH | A
WT PTH | B
KO VEH | C
WT VEH | C
Groups not connected by the same letter are different

C

2W ANOVA | Prob>ltl
GENOTYPE | <0.0001
TREATMENT | <0.0001
TREAT X GENE | 0.01
TUKEY HSD
WT VEH | A
KO VEH | B
WT PTH | B
KO PTH | C
Groups not connected by the same letter are different

D

2W ANOVA | Prob>ltl
GENOTYPE | 0.002
TREATMENT | <0.0001
TREAT X GENE | <0.0001
TUKEY HSD
KO PTH | A
WT PTH | B
WT VEH | B
KO VEH | B
Groups not connected by the same letter are different

E

2W ANOVA | Prob>ltl
GENOTYPE | <0.0001
TREATMENT | <0.0001
TREAT X GENE | 0.09

F

2W ANOVA | Prob>ltl
GENOTYPE | <0.0001
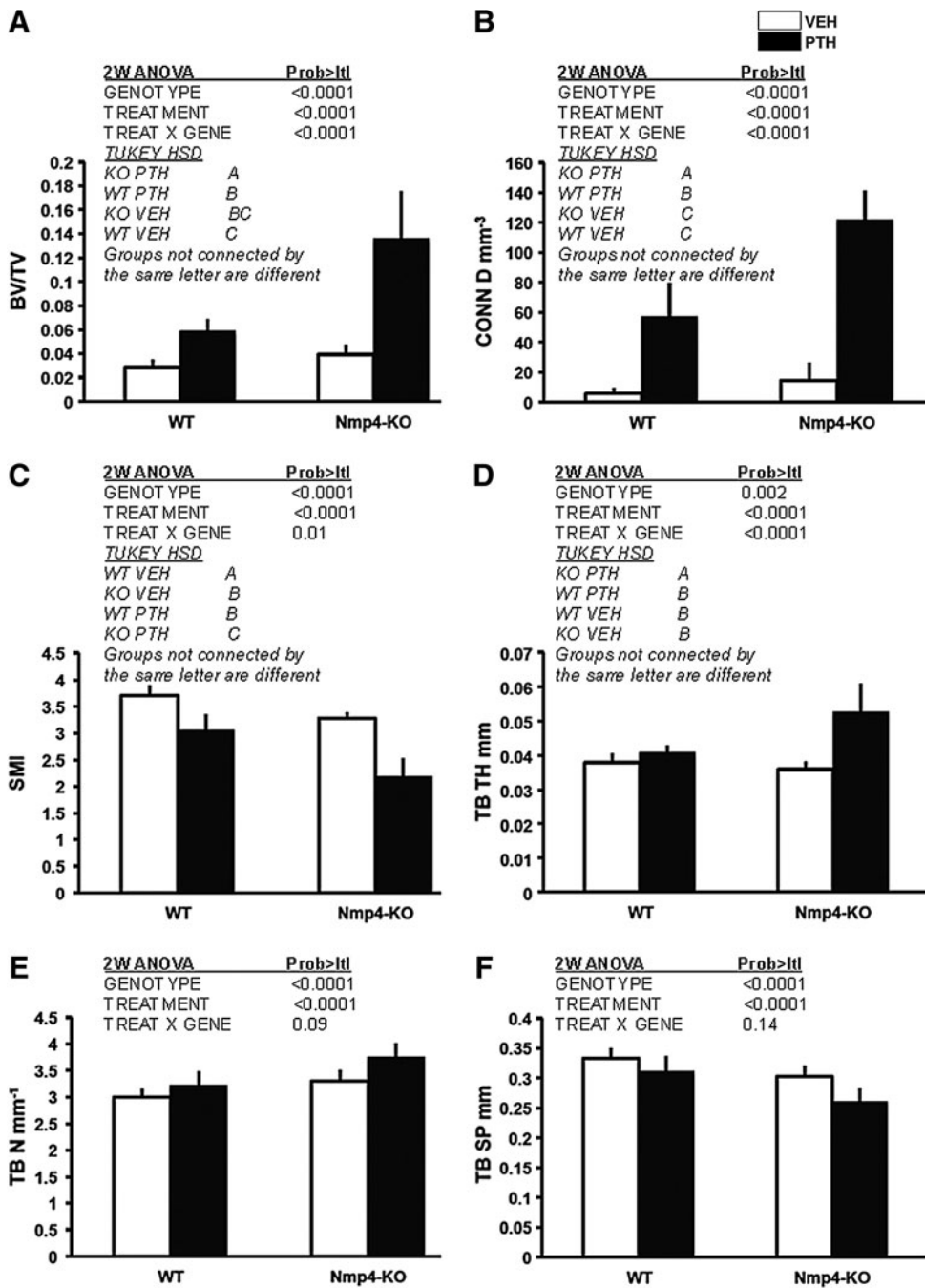TREATMENT | <0.0001
TREAT X GENE | 0.14

FIG. 1. Disabling Nmp4 enhanced PTH-induced increases in femoral cancellous bone after 3 weeks of treatment. Microcomputed tomography-acquired femoral trabecular architecture, including **(A)** BV/TV%; **(B)** Conn D mm^{-3}; **(C)** SMI; **(D)** Tb.Th mm: **(E)** Tb.N mm^{-1}: **(F)** Tb.Sp mm was compared between WT and *Nmp4*-KO mice that had been treated with intermittent hPTH (1–34) 30 μg/kg/day or vehicle for 3 weeks (average±SD, number of mice/experimental group=10). Statistical differences were determined using a 2-way ANOVA. A Tukey's HSD post hoc test was used to determine differences between the treatment groups if a significant genotype×treatment interaction was indicated, and there was such an interaction for BV/TV, Conn D, SMI, and Tb.Th. HSD, honestly significant difference; PTH, parathyroid hormone; VEH, vehicle; SMI, structure model index; Tb.N, trabecular number; Tb.Th, trabecular thickness; Tb.Sp, trabecular spacing; WT, wild type; KO, knockout.

from the *Nmp4*-null BM as compared to the WT BM (Fig. 2C). There was a trend toward increased yield of CFU-F and CFU-F$^{AlkPhos+}$ cells with PTH treatment in both genotypes, but this was not significant. Therefore, we next addressed whether the frequency of the self-renewing multipotent mesenchymal stem cell (CD45–/CD146+/CD105+/nestin+), the precursor of CFU-F-derived lineages, including osteoprogenitors, is elevated in untreated *Nmp4*-KO mice. Indeed, we observed a nearly 4-fold increase in this cell phenotype in the null BM (Fig. 2D).

Nmp4 has no significant influence on the percentage of CD4+ T cells in the BM or PBL (Table 2), but recent studies have demonstrated that CD8+ T cells play an obligatory role in the PTH anabolic response via their release of the glyco-

protein Wnt10b, a potent agonist for osteoprogenitors [19,20]. Indeed, the present data show that the percentage of CD8+ T cells in the null BM was 2-fold greater than that observed in the WT BM (Fig. 3A), but there was no difference in the percent CD8+ T cells in the PBL between the genotypes (Fig. 3B). Additionally, PTH treatment had no effect on the size of this population of cells in either the BM or PBL.

Next, to address whether the observed modest elevation in bone resorption in the null mice and the enhanced number of osteoclasts derived from their BM [7] is due, in part, to an increase in osteoclast progenitors, we evaluated the number of CFU-GM cells from our treatment groups. Indeed, the *Nmp4*-null mice exhibited a modest (∼1.6-fold), but significant, increase in CFU-GM cells as compared to their WT

| | WT | | KO | | 2-Way ANOVA P values | | |
	VEH	PTH	VEH	PTH	Genotype	Treatment	Gene × Treat
Cellularity (10^6/femur)	9.1 ± 6.2	8.1 ± 5.6	14.3 ± 7.1	11.5 ± 6.6	0.04	0.33	0.64
% Spleen weight	0.40 ± 0.03	0.47 ± 0.06	0.42 ± 0.08	0.46 ± 0.07	0.84	0.01	0.49
WBC (K/μL)	4.8 ± 1.1	4.9 ± 1.4	4.5 ± 1.6	5.6 ± 1.6	0.70	0.16	0.24
NE (K/μL)	0.70 ± 0.28	0.62 ± 0.40	0.56 ± 0.32	0.73 ± 0.33	0.86	0.67	0.22
NE%	14.2 ± 3.3	12.6 ± 6.1	12.7 ± 5.7	12.8 ± 4.7	0.88	0.33	0.82
LY (K/μL)	1.0 ± 0.78	4.1 ± 1.1	3.7 ± 1.4	4.8 ± 1.3	0.62	0.11	0.26
LY%	82.4 ± 4.3	83.8 ± 5.9	82.2 ± 8.1	84.4 ± 4.8	0.88	0.33	0.82
MO (K/μL)	0.13 ± 0.05	0.14 ± 0.06	0.16 ± 0.09	0.12 ± 0.03	0.89	0.53	0.21
MO%	2.7 ± 0.87	2.9 ± 1.0	3.6 ± 2.1	2.2 ± 0.53	0.69	0.15	0.06
EO (IC/μL)	0.03 ± 0.05	0.03 ± 0.04	0.04 ± 0.05	0.02 ± 0.03	0.92	0.49	0.54
EO%	0.54 ± 0.88	0.56 ± 0.53	1.17 ± 1.57	0.43 ± 0.52	0.42	0.24	0.23
RBC (M/μL)	9.6 ± 0.46	9.1 ± 1.5	8.6 ± 1.2	8.8 ± 1.4	0.09	0.67	0.38
PLT (K/μL)	493.8 ± 124.7	486.6 ± 167.4	378.9 ± 207.9	487.5 ± 142.8	0.27	0.32	0.26

WT and null mice were treated with intermittent PTH or vehicle for 3 weeks (number of mice/experimental group = 9–14). A 2-factor ANOVA was used to evaluate the impact of genotype and treatment on the individual parameters. Statistical significance was set at $P < 0.01$ to guard against type I errors. Percent (%) spleen weight is the weight of the organ divided by the total body weight.

WT, wild type; VEH, vehicle; PTH, parathyroid hormone; KO, knockout; ANOVA, analysis of variance; EO, eosinophils; LY, lymphocytes; MO, monocytes; NE, neutrophils; PLT, platelets; RBC, red blood cell; WBC, white blood cells.

littermates (Fig. 4). PTH had no effect on the number of these cells (Fig. 4).

Discussion

A significant drawback to the use of PTH as an osteoporosis drug is that its anabolic potency declines within a relatively short period of time, which is particularly problematic in treating a chronic degenerative disease [21]. The cellular and molecular mechanisms underlying this closing of the PTH anabolic window are unknown. We have recently determined that deleting the transcription factor Nmp4/CIZ from mice significantly extends the PTH anabolic window and results in enhanced trabecular bone formation without compromising hormone-stimulated gains in cortical bone [7,8].

An intriguing aspect of the Nmp4-KO mouse response to anabolic doses of PTH is that the enhanced addition of trabecular bone requires a lag period to materialize [7]. Previously, we reported that both WT and null mice exhibited equivalent PTH-stimulated increases in trabecular bone during the first 2 weeks of a 7-week treatment. In this study, we compared hormone-induced increases in femoral cancellous bone after 3 weeks of treatment and indeed observed that the Nmp4-KO mice exhibited a >2-fold increase in PTH-induced accrual of femoral trabecular bone formation as compared to their WT littermates. This enhanced response to PTH was manifested in an augmented increase in BV/TV, trabecular connectivity (Conn D), and trabecular thickness (Tb.Th). Additionally, PTH had a greater impact on the SMI in the null mice. A decrease in SMI indicates a change in cancellous architecture from a rod-like to a plate-like

| | WT | | KO | | 2-Way ANOVA P values | | |
Units (%)	VEH	PTH	VEH	PTH	Genotype	Treatment	Gene × Treat
Pre-B (BM)	11.6 ± 7.2	12.1 ± 7.0	7.6 ± 4.7	9.7 ± 5.7	0.08	0.45	0.65
Pre-B (PBL)	17.5 ± 6.5	20.0 ± 7.8	11.7 ± 6.5	16.9 ± 7.6	0.04	0.06	0.52
Immature B (BM)	5.9 ± 1.3	6.3 ± 2.7	6.8 ± 3.5	6.3 ± 4.4	0.64	0.95	0.65
Immature B (PBL)	20.7 ± 10.9	22.3 ± 8.5	25.1 ± 11.3	22.8 ± 11.6	0.43	0.90	0.54
Mature B (BM)	3.5 ± 3.5	3.5 ± 3.7	3.0 ± 3.0	3.5 ± 3.4	0.81	0.75	0.79
Mature B (PBL)	5.7 ± 3.8	5.5 ± 4.8	7.2 ± 6.7	8.3 ± 6.7	0.20	0.79	0.68
CD4 + T (BM)	1.6 ± 0.39	1.4 ± 0.40	1.9 ± 0.74	2.0 ± 1.0	0.03	0.73	0.36
CD4 + T (PBL)	15.8 ± 2.5	15.6 ± 4.3	16.3 ± 5.5	17.1 ± 3.7	0.41	0.79	0.68
Myeloid (BM)	34.5 ± 5.7	36.4 ± 4.8	32.0 ± 7.6	34.1 ± 11.2	0.30	0.38	0.97
Myeloid (PBL)	6.0 ± 2.5	5.3 ± 1.3	5.9 ± 2.9	7.4 ± 4.4	0.24	0.65	0.22
LSK (BM)	0.11 ± 0.06	0.11 ± 0.06	0.12 ± 0.14	0.26 ± 0.22	0.05	0.07	0.09
L5K (PBL)	0.03 ± 0.03	0.03 ± 0.03	0.03 ± 0.04	0.02 ± 0.03	0.60	0.95	0.92

Mice were treated with PTH or vehicle for 3 weeks (number of mice/experimental group = 11–14). Statistical significance was set at $P < 0.0l$. LSK, lin-/Scal+/c-Kit+; BM, bone marrow; PBL, peripheral blood.

TABLE 3. CLONOGENIC ASSAYS OF WT AND NMP4-KO MICE AS DESCRIBED IN THE MATERIALS AND METHOD SECTION

Units: colony/femur	WT		KO		2-Way ANOVA P values		
	VEH	PTH	VEH	PTH	Genotype	Treatment	Gene × Treat
CFU-C	27307 ± 13080	31311 ± 17107	44898 ± 22460	40573 ± 27265	0.04	0.98	0.52
CFU-G	1145 ± 2204	936 ± 1402	560 ± 998	284 ± 460	0.12	0.54	0.93
CFU-GEMM	941 ± 1219	762 ± 830	1065 ± 1817	847 ± 987	0.78	0.61	0.96
CFU-M	7409 ± 4316	9405 ± 7227	11229 ± 6172	9629 ± 6478	0.27	0.91	0.33

WT and null mice were treated with intermittent PTH or vehicle for 3 weeks (number of mice/experimental group = 10–14). A 2-factor ANOVA was used to evaluate the impact of genotype and treatment on the individual parameters. Statistical significance was set at $P < 0.01$ to guard against type I errors.

morphology and is a result of alterations in modeling and remodeling [18,22,23]. This suggests that PTH-stimulated increases in bone strength are enhanced in the *Nmp4*-KO mice, although this must be confirmed by biomechanical testing.

Our data indicate that deleting Nmp4/CIZ establishes a BM microenvironment that is primed for anabolic signals. We observed no differences in femur cellularity, % spleen weight, or in the profiles of the vast majority of blood elements; however, there was a striking difference in the number of osteoprogenitor cells as evaluated by the clonogenic CFU-F$^{AlkPhos+}$ assay. The *Nmp4*-null BM yielded 4-fold more of these colonies than did the WT BM. In an earlier study, Noda and colleagues observed that BM cultures from null mice yielded about 3-fold more mineralized nodules than WT mice [24], which is equivalent to measuring CFU–osteoblast colonies [25]. In the present study, we also determined that the total number of CFU-F colonies obtained from the null mice was significantly elevated as was the% CFU-F$^{AlkPhos+}$/total CFU-F. These data together suggest that Nmp4 suppresses the frequency of CFU-F cells and impedes commitment to the osteogenic lineage. This is consistent with the elevated number of CD45−/CD146+/CD105+/nestin+ cells obtained in the *Nmp4*-KO mice. These cells are self-renewing multipotent mesenchymal stem cells and contain all the bone marrow colony-forming-unit fibroblastic colony activity [26,27]. PTH did not significantly impact the number of CFU-F$^{AlkPhos+}$ colonies recovered from the BM of either genotype, although there was a trend toward modestly elevating the frequency of these cells. A variety of studies have shown conflicting stimulatory and inhibitory effects of PTH on osteoprogenitor proliferation [28–30]; however, the
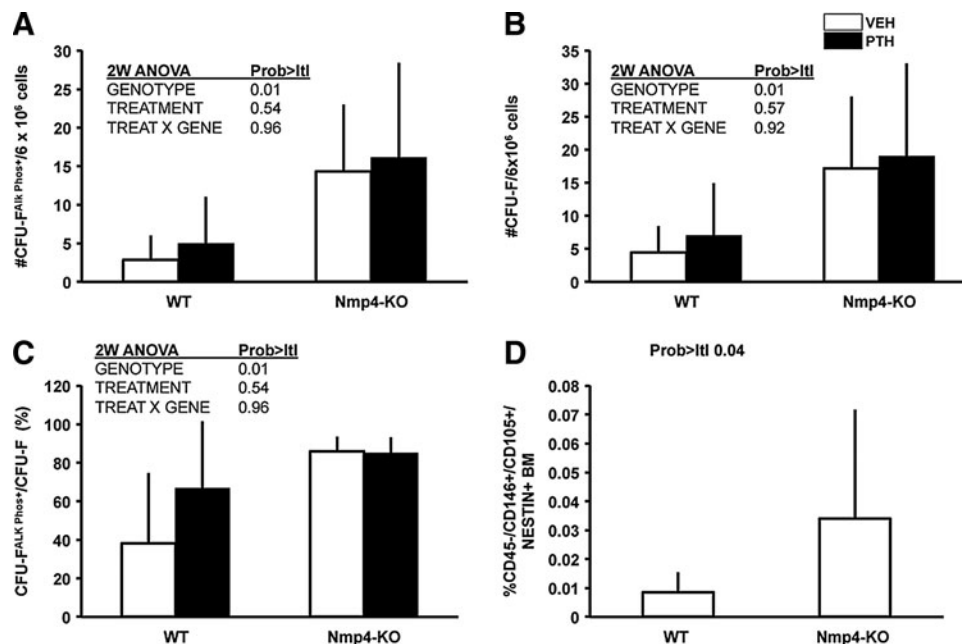

FIG. 2. *Nmp4*-KO BM yielded more osteogenic stem and progenitor cells irrespective of treatment. **(A)** Total number of CFU-F$^{AlkPhos+}$ colonies in BM cultures derived from WT and *Nmp4*-KO mice treated with intermittent hPTH (1–34) 30 μg/kg/day or vehicle for 3 weeks. **(B)** Total number of CFU-F colonies. **(C)** The percent CFU-F$^{AlkPhos+}$ colonies/total CFU-F colonies (average ± SD, number of mice/experimental group = 6–8; statistical differences determined by a 2-way ANOVA). **(D)** The frequency of femoral CD45−/CD146+/CD105+/nestin+ multipotent mesenchymal stem cells in untreated WT and *Nmp4*-KO mice; FACS was used to evaluate the BM from each mouse as described in the Materials and Methods section (average ± SD, number of mice/experimental group = 12–20; statistical difference was determined using a 2-sample *t*-test assuming unequal variances). BM, bone marrow; FACS, fluorescence activated cell sorting.
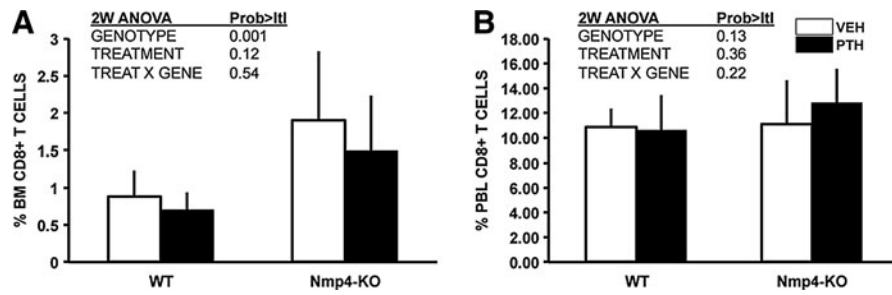
FIG. 3. *Nmp4*-KO BM harbored more CD8+ T cells than WT BM irrespective of treatment. **(A)** FACS analysis showed that there were significantly more CD8+ T cells in the BM of *Nmp4*-KO mice as compared to that observed in WT mice. **(B)** No differences between WT and *Nmp4*-KO mice in CD8+ T cells were detected in the PBL (average±SD, number of mice/ experimental group 11–14; statistical differences were determined using a 2-way ANOVA). PBL, peripheral blood.

prevailing view is that intermittent PTH recruits osteopro-genitors into the osteoblast differentiation pathway and enhances their survival instead of increasing the size of this progenitor pool [31, and references therein]. It is the accumulation of repeated new waves of osteoprogenitors with enhanced osteogenic potential that mediates the PTH-stimulated increase in bone mass [28,32]. This may also explain that the observed lag period before the enhanced PTH-induced bone formation phase is initiated in the *Nmp4*-null mice. If indeed the anabolic effect of intermittent PTH is the result of consecutive waves of committed osteoblast differentiation accumulated from each PTH exposure, in which hormone only acts on the BM early osteoprogenitor cells [28], then the rate of PTH osteoprogenitor recruitment would be equivalent in both the WT and KO mice, but the WT osteoprogenitor pool would be depleted before the KO population. This is consistent with the observed equivalent addition of bone during the first 2 weeks of treatment, but the divergence in both serum osteocalcin and bone formation in the null mice at 3 weeks [7 and the present work]. Finally, the *Nmp4/CIZ*-KO osteoblast exhibits a modest, but significant, enhanced response to numerous anabolic stimuli, including PTH, BMP2, and mechanical loading [24,33–35];

therefore, an expanded population of such cells is certainly consistent with the augmented skeletal bone mineral density and bone mineral content of the null animals.

The expanded *Nmp4*-KO osteoprogenitor pool may be supported by the 2-fold increase in BM CD8+ T cells as compared to the WT mice. CD8+ T cells express the PTH receptor PTHR1 and support intermittent hormone anabolic activity via their secretion of the glycoprotein Wnt10b, a potent agonist of osteoblast activity [19,20]. PTH-induced bone formation was significantly reduced in T-cell-deficient mice and in these mice reconstituted with *Wnt10b*$^{-/-}$ T cells [20]. Interestingly, we observed no difference in the level of CD8+ T cells in the PBL, suggesting that the recruitment and/or the retention of these cells is enhanced in the null BM microenvironment. BM CD8+ T cells consist chiefly (∼50%) of CCR7+ L-selectin+central memory cells [36], and the mechanisms underlying this concentration in the marrow involve PSGL-1-mediated rolling and VCAM-1-VLA-4-mediated arrest in BM venules [36]. The retention of these cells may be enhanced by CXCL12 (a ligand for CXCR4 on central memory T cells) [36]. Finally, IL15-dependent homeostatic proliferation of memory T cells contributes to their disproportionate presence in the BM [37,38]. Whether the null BM microenvironment is enriched in these various cytokines and/or selectin ligands and adhesion molecules remains to be determined.
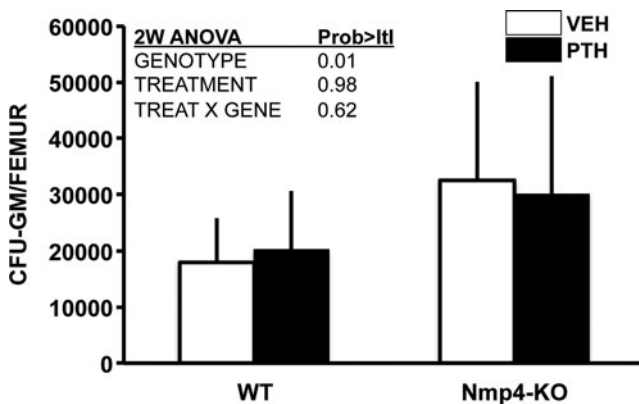
A second provocative aspect of the *Nmp4*-KO skeletal phenotype is that the baseline bone mineral density and bone mineral content are slightly increased despite a modest elevation of bone resorption [7]. While the increase in osteoclast number may be attributed to coupling (eg, increased osteoblast support of an increase in osteoclasto-genesis [14 and references therein]), the present data suggest that this reflects intrinsic differences in osteoclast progenitor populations. We observed a modest (1.6-fold), but statistically significant, increase in CFU-GM cells in the null mice as compared to their WT counterparts. Although CFU-C cells were elevated in the *Nmp4*-KO mice, this only approached significance, and there was no difference in the levels of CFU-M cells between the genotypes. The precise lineage of the osteoclast and its relationship to other hematopoietic cells is controversial; however, there are a number of studies supporting the hypothesis that the osteoclast lineage branches to terminal differentiation via the CFU-GM cells before further passage toward the mono-cyte/macrophage lineage [39,40].

FIG. 4. More CFU-GM cells were obtained from *Nmp4*-KO mice than WT mice, irrespective of treatment. Intermittent hPTH (1–34) 30 μg/kg/day or vehicle was administered for 3 weeks as described in the Materials and Methods section (average±SD, number of mice/experimental group = 10–14; statistical differences were determined using a 2-way ANOVA).

The present data suggest that the heightened bone anabolism and modestly elevated bone resorption in the global *Nmp4*-KO mouse are derived, in part, from a unique confluence of BM stem, progenitor, and blood cells. The null BM harbors an expanded pool of MSCs (CD146 + /nestin +), osteoprogenitors, and CD8 + T cells, which together supply the osteoblasts necessary for the observed augmented bone-forming activity, even in the presence of elevated bone resorption driven by the modestly enlarged CFU-GM pool (1.6-fold) that contributes to the osteoclasts. This may support an environment of enhanced anabolic remodeling.

Our data do not directly relate the differences in cellular composition observed in the *Nmp4*-KO mice to enhanced PTH-stimulated increases in trabecular architecture. To address this issue, a combination of genetic-, drug-, and transplantation-based approaches will be required, because all of these methods have strengths and drawbacks, yet their intersection reveals complementary aspects of the phenomenon under study. However, the previously observed heightened PTH-responsiveness and osteogenic capacity of *Nmp4*-KO BMSCs and osteoblasts in culture [24,33,35] and the enhanced number of the progenitors of these cells (present study) likely make a substantial contribution to the extended anabolic window. Additionally, Nmp4/CIZ deficiency augmented newly formed trabecular bone mass after femoral BM ablation as compared to WT mice [24], confirming the enhanced osteogenic capacity of the reconstituted KO BM. It is certainly tenable that multiple stem/progenitor types are necessary for maintaining an open PTH anabolic window, and that one transcription factor has significant direct and/or indirect control over these populations was unexpected despite the fact that Nmp4/CIZ is expressed in multiple cell and tissue types [41]. Nmp4/CIZ has been proposed as a potential target for osteoporosis therapy, [42] and the present data further develop this idea, suggesting that disabling Nmp4/CIZ may provide an adjuvant therapy for extending PTH clinical efficacy by expanding the stem/progenitor populations sustaining its anabolic action.

Acknowledgments

Author Disclosure Statement

No competing financial interests exist.

References

1. Trivedi R, R Goswami and N Chattopadhyay. (2010). Investigational anabolic therapies for osteoporosis. Expert Opin Investig Drugs 19:995–1005.
2. Cusano NE and JP Bilezikian. (2011). Combination anti-resorptive and osteoanabolic therapy for osteoporosis: we are not there yet. Curr Med Res Opin 27:1705–1707.
3. Cusano NE and JP Bilezikian. (2010). Teriparatide: variations on the theme of a 2-year therapeutic course. IBMS Bone Key 7:84–87.
4. Bilezikian JP. (2008). Combination anabolic and anti-resorptive therapy for osteoporosis: opening the anabolic window. Curr Osteoporos Rep 6:24–30.
5. Cosman F, J Nieves, M Zion, L Woelfert, M Luckey and R Lindsay. (2005). Daily and cyclic parathyroid hormone in women receiving alendronate. N Engl J Med 353: 566–575.
6. Silverman S and C Christiansen. (2012). Individualizing osteoporosis therapy. Osteoporos Int 23:797–809.
7. Childress P, BK Philip, AG Robling, A Bruzzaniti, MA Kacena, N Bivi, LI Plotkin, A Heller and JP Bidwell. (2011). Nmp4/CIZ suppresses the response of bone to anabolic parathyroid hormone by regulating both osteoblasts and osteoclasts. Calcif Tissue Int 89:74–89.
8. Robling AG, P Childress, J Yu, J Cotte, A Heller, BK Philip and JP Bidwell. (2009). Nmp4/CIZ suppresses parathyroid hormone-induced increases in trabecular bone. J Cell Physiol 219:734–743.
9. Satija NK, GU Gurudutta, S Sharma, F Afrin, P Gupta, YK Verma, VK Singh and RP Tripathi. (2007). Mesenchymal stem cells: molecular targets for tissue engineering. Stem Cells Dev 16:7–23.
10. Qin L, J Tamasi, L Raggatt, X Li, JH Feyen, DC Lee, E Dicicco-Bloom and NC Partridge. (2005). Amphiregulin is a novel growth factor involved in normal bone development and in the cellular response to parathyroid hormone stimulation. J Biol Chem 280:3974–3981.
11. Bozec A, L Bakiri, A Hoebertz, R Eferl, AF Schilling, V Komnenovic, H Scheuch, M Priemel, CL Stewart, M Amling, and EF Wagner. (2008). Osteoclast size is controlled by Fra-2 through LIF/LIFreceptorsignalling and hypoxia. Nature 454:221–225.
12. Karreth F, A Hoebertz, H Scheuch, R Eferl and EF Wagner. (2004). The AP1 transcription factor Fra2 is required for efficient cartilage development. Development 131:5717–5725.
13. Qin L, LJ Raggatt, and Partridge. (2004). Parathyroid hormone: a double-edged sword for bone metabolism. Trends Endocrinol Metab 15:60–65.
14. Kular J, J Tickner, SM Chim and J Xu. (2012). An overview of the regulation of bone remodelling at the cellular level. Clin Biochem 45:863–873.
15. Nishida S, A Yamaguchi, T Tanizawa, N Endo, T Mashiba, Y Uchiyama, T Suda, S Yoshiki and HE Takahashi. (1994). Increased bone formation by intermittent parathyroid hormone administration is due to the stimulation of proliferation and differentiation of osteoprogenitor cells in BM. Bone 15:717–723.
16. Yang FC, S Watanabe, K Tsuji, MJ Xu, A Kaneko, Y Ebihara and T Nakahata. (1998). Human granulocyte colony-stimulating factor (G-CSF) stimulates the in vitro and in vivo development but not commitment of primitive multipotential progenitors from transgenic mice expressing the human G-CSF receptor. Blood 92:4632–4640.
17. Niziolek PJ, S Murthy, SN Ellis, KB Sukhija, TA Hornberger, CH Turner and AG Robling. (2009). Rapamycin impairs trabecular bone acquisition from high-dose but not low-dose intermittent parathyroid hormone treatment. J Cell Physiol 221:579–585.
18. Ding M and I Hvid. (2000). Quantification of age-related changes in the structure model type and trabecular thickness of human tibial cancellous bone. Bone 26:291–295.
19. Bedi B, JY Li, H Tawfeek, KH Baek, J Adams, SS Vangara, MK Chang, M Kneissel, MN Weitzmann and R Pacifici. (2012). Silencing of parathyroid hormone (PTH) receptor 1 in

T cells blunts the bone anabolic activity of PTH. Proc Natl Acad Sci U S A 109:E725–E733.

20. Terauchi M, JY Li, B Bedi, KH Baek, H Tawfeek, S Galley, L Gilbert, MS Nanes, M Zayzafoon, et al. (2009). T lymphocytes amplify the anabolic activity of parathyroid hormone through Wnt10b signaling. Cell Metab 10:229–240.

21. Baron R and H Hesse. (2012). Update on bone anabolics in osteoporosis treatment: rationale, current status, and perspectives. J Clin Endocrinol Metab 97:311–325.

22. Allen MR and DB Burr. (2006). Parathyroid hormone and bone biomechanics. Clin Rev Bone Miner Metab 4:259–268.

23. Riggs BL and AM Parfitt. (2005). Drugs used to treat osteoporosis: the critical need for a uniform nomenclature based on their action on bone remodeling. J Bone Miner Res 20:177–184.

24. Morinobu M, T Nakamoto, K Hino, K Tsuji, ZJ Shen, K Nakashima, A Nifuji, H Yamamoto, H Hirai and M Noda. (2005). The nucleocytoplasmic shuttling protein CIZ reduces adult bone mass by inhibiting bone morphogenetic protein-induced bone formation. J Exp Med 201:961–970.

25. Owen M and AJ Friedenstein. (1988). Stromal stem cells: marrow-derived osteogenic precursors. Ciba Found Symp 136:42–60.

26. Méndez-Ferrer S, TV Michurina, F Ferraro, AR Mazloom, BD Macarthur, SA Lira, DT Scadden, A Ma'ayan, GN Enikolopov and PS Frenette. (2010). Mesenchymal and haematopoietic stem cells form a unique bone marrow niche. Nature 466:829–834.

27. Sacchetti B, A Funari, S Michienzi, S Di Cesare, S Piersanti, I Saggio, E Tagliafico, S Ferrari, PG Robey, M Riminucci and P Bianco. (2007). Self-renewing osteoprogenitors in bone marrow sinusoids can organize a hematopoietic microenvironment. Cell 131:324–336.

28. Wang YH, Y Liu and DW Rowe. (2007). Effects of transient PTH on early proliferation, apoptosis, and subsequent differentiation of osteoblast in primary osteoblast cultures. Am J Physiol Endocrinol Metab 292:E594–E603.

29. Onyia JE, B Miller, J Hulman, J Liang, R Galvin, C Frolik, S Chandrasekhar, AK Harvey, J Bidwell, J Herring and JM Hock. (1997). Proliferating cells in the primary spongiosa express osteoblastic phenotype in vitro. Bone 20:93–100.

30. Isogai Y, T Akatsu, T Ishizuya, A Yamaguchi, M Hori, N Takahashi and T Suda. (1996). Parathyroid hormone regulates osteoblast differentiation positively or negatively depending on the differentiation stages. J Bone Miner Res 11:1384–1393.

31. Jilka RL. (2007). Molecular and cellular mechanisms of the anabolic effect of intermittent PTH. Bone 40:1434–1446.

32. Wang YH, Y Liu, K Buhl and DW Rowe. (2005). Comparison of the action of transient and continuous PTH on primary osteoblast cultures expressing differentiation stage-specific GFP. J Bone Miner Res 20:5–14.

33. Alvarez MB, P Childress, BK Philip, R Gerard-O'Riley, M Hanlon, BS Herbert, AG Robling, FM Pavalko and JP Bidwell. (2012). Immortalization and characterization of osteoblast cell lines generated from wild-type and Nmp4-null mouse BM stromal cells using murine telomerase reverse transcriptase (mTERT). J Cell Physiol 227:1873–1882.

34. Yang Z, JP Bidwell, SR Young, R Gerard-O'Riley, H Wang and FM Pavalko. (2010). Nmp4/CIZ inhibits mechanically induced beta-catenin signaling activity in osteoblasts. J Cell Physiol 223:435–441.

35. Shen ZJ, T Nakamoto, K Tsuji, A Nifuji, K Miyazono, T Komori, H Hirai and M Noda. (2002). Negative regulation of bone morphogenetic protein/Smad signaling by Cas-interacting zinc finger protein in osteoblasts. J Biol Chem 277:29840–29846.

36. Mazo IB, M Honczarenko, H Leung, LL Cavanagh, R Bonasio, W Weninger, K Engelke, L Xia, RP McEver, PA Koni, LE Silberstein, UH von Andrian. (2005). BM is a major reservoir and site of recruitment for central memory CD8+ T cells. Immunity 22:259–270.

37. Herndler-Brandstetter D, K Landgraf, B Jenewein, A Tzankov, R Brunauer, S Brunner, W Parson, F Kloss, R Gassner, G Lepperdinger and B Grubeck-Loebenstein. (2011). Human BM hosts polyfunctional memory CD4+ and CD8+ T cells with close contact to IL-15-producing cells. J Immunol 186:6965–6971.

38. Becker TC, SM Coley, EJ Wherry and R Ahmed. (2005). BM is a preferred site for homeostatic proliferation of memory CD8 T cells. J Immunol 174:1269–1273.

39. Hodge JM, MA Kirkland, CJ Aitken, CM Waugh, DE Myers, CM Lopez, BE Adams and GC Nicholson. (2004). Osteoclastic potential of human CFU-GM: biphasic effect of GM-CSF. J Bone Miner Res 19:190–199.

40. Menaa C, N Kurihara and GD Roodman. (2000). CFU-GM-derived cells form osteoclasts at a very high efficiency. Biochem Biophys Res Commun 267:943–946.

41. Thunyakitpisal P, M Alvarez, K Tokunaga, JE Onyia, J Hock, N Ohashi, H Feister, SJ Rhodes and JP Bidwell. (2001). Cloning and functional analysis of a family of nuclear matrix transcription factors (NP/NMP4) that regulate type I collagen expression in osteoblasts. J Bone Miner Res 16:10–23.

42. Krane SM. (2005). Identifying genes that regulate bone remodeling as potential therapeutic targets. J Exp Med 201:841–843.

Address correspondence to:
Dr. Feng-Chun Yang
Department of Pediatrics
Indiana University School of Medicine
R4-427, 1044 West Walnut Street
Indianapolis, IN 46202

E-mail: fyang@iupui.edu

Dr. Joseph P. Bidwell
Department of Anatomy & Cell Biology
Indiana University School of Medicine
Medical Science Building 5035
635 Barnhill Drive
Indianapolis, IN 46202

E-mail: jbidwell@iupui.edu